

Low-Thrust Trajectories to Jupiter via Gravity Assists from Venus, Earth, and Mars

Masataka Okutsu,¹ Chit Hong Yam,¹ and James M. Longuski.²
Purdue University, West Lafayette, Indiana 47907-2023

We design low-thrust gravity-assist trajectories to Jupiter via gravity assists from Venus, Earth, and Mars. Trades between time of flight, mass, and hardware specifications are examined for various flyby bodies such as Mars, Earth, Venus-Earth, and Venus-Venus. We find (locally) propellant-optimal trajectories for ranges of specific impulse and specific mass that represent present-day technologies (such as an ion thruster with a radioisotope power source) and future technologies (such as a nuclear-powered magnetoplasmadynamic thruster which may be available in 10 to 15 years). We consider the 35-year launch period from January 2010 to December 2044.

I. Introduction

THE Galileo spacecraft which orbited Jupiter from 1995 to 2003 observed intense volcanic activities on Io and collected evidence that there may be oceans beneath the surfaces of Europa, Ganymede, and Callisto. The icy subsurface oceans of Europa is believed to be the largest body of water in our solar system, making this moon a prime destination in a search for life beyond Earth. As mission designers continue to explore trajectory options to Jupiter, the proven technique of gravity assist, which has enabled and enhanced numerous missions, will likely play a role in future missions. Whereas Petropoulos et al.¹ identify numerous ballistic trajectories that are attractive for missions to Jupiter, the design space of trajectories is further expanded by advances in electric propulsion. Despite of its low level of thrust, electric propulsion can accelerate a spacecraft to a high speed over a sufficiently long period of time. Of primary interest are missions that could combine the benefit of electric propulsion and gravity assists.

The design space of low-thrust, gravity-assist trajectories is large: considering missions to Jupiter with up to three gravity assists, including such paths as Earth-Jupiter (direct), Earth-Venus-Jupiter, Earth-Earth-Mars-Jupiter and Earth-Venus-Earth-Earth-Jupiter, there are $1+3+3^2+3^3 = 40$ possible paths to Jupiter via gravity assists from Venus, Earth and Mars; 121 paths if up to four flybys is considered. Furthermore, low-thrust trajectories can have more than one locally optimal trajectory near the launch date, because trajectories can have different number of revs for the same time of flight (TOF). If the TOF is allowed to vary, then we will find a family of locally optimal solutions associated with the range of TOF. In Refs. 2-4 Parcher and Sims examine such trades between the final mass and TOF for a number of paths to Jupiter for Earth launch in the years 2011 and 2012.

Unlike conic trajectories, in which a propellant-optimal solution is identical regardless of the size of the spacecraft, the characteristics of the low-thrust trajectories and electric-propulsion hardware are tightly coupled. Thus, different types of spacecraft, for example, a small radioisotope-powered spacecraft with an ion thruster and a large nuclear-powered spacecraft with a magnetoplasmadynamic (MPD) thruster, will likely fly different trajectories. Our objective is then to design trajectories to Jupiter and study how trajectory characteristics vary when subject to variations in TOF and hardware parameters. We focus our study on nuclear electric propulsion (NEP), in which, unlike in the case for the solar electric propulsion (SEP), the power level can be maintained regardless of its distance from the sun. Nuclear power enables not only years of scientific investigations at this far-from-sun planet but also rendezvous via electric propulsion upon arriving to Jupiter, eliminating the need for a large arrival insertion maneuver by a chemical stage which may be necessary in the case of SEP.

With the objective of rendezvous in mind, cases considered in this paper achieve zero arrival V_∞ at Jupiter. We use Jupiter Icy Moons Orbiter (JIMO)⁵⁻⁹ hardware parameters to allow comparisons with previous studies.⁹ Table 1 shows representative parameters for the JIMO spacecraft with a reactor of 100-kWe class. The Earth departure mass is 20,000 kg when the launch V_∞ is zero. (For a given launch vehicle with a specified LEO payload capability, injected mass to the interplanetary trajectory reduces if greater launch energy is required, because more of the LEO payload must be used for the upper-stage mass.) Because our spacecraft mass is so large (i.e. the mass of the JIMO

¹ Doctoral Candidate, School of Aeronautics and Astronautics, 315 N. Grant St., Student Member AIAA.

² Professor, School of Aeronautics and Astronautics, 315 N. Grant St., Associate Fellow AIAA, Member AAS.

spacecraft), we assume a fictitious launch vehicle twice the LEO-payload capability of the Delta IV Heavy launch vehicle.

Table 1 Representative Hardware Parameters for the JIMO Spacecraft

Parameter	Values
Power Available to the Thrusters, P	95 kW
Specific Impulse, I_{sp}	6,000 s
Overall Efficiency, η	70 %
Thrust, T	2.26 N
Mass Flow Rate, \dot{m}	38.4 mg/s
Injected Mass at Zero Launch V_{∞} , m_0	20,000 kg

The type of engine typically considered for NEP missions to Jupiter is ion propulsion. (Ion propulsion was successfully demonstrated by the Deep Space 1 spacecraft,¹⁰ which was launched in 1998 and performed flybys of an asteroid and a comet.) The propulsion system considered for JIMO is an improved version of the NSTAR engine of the Deep Space 1 spacecraft.¹⁰ Although ion thrust is a promising choice for interplanetary missions, there are a number of engines (electrothermal, electrostatic, and electromagnetic) with wide ranges of specific impulse, overall efficiency, thrust density, technological maturity, and power levels. We investigate the impact of these spacecraft parameters on low-thrust trajectories.

II. Design Method

Relatively few studies have been published on how to obtain an initial guess for optimization of low-thrust, gravity-assist trajectories. In this paper we make use two types of initial guesses: exponential-sinusoid arcs in the “shape-based method” and conic arcs in the “continuation method.”

In the shape-based method, proposed by Petropoulos and Longuski,¹¹⁻¹⁴ a low-thrust trajectory is assumed to follow the shape of exponential sinusoids, defined by parameters specified by a mission designer. Such low-thrust arcs patched together with conic arcs at the gravity-assist bodies serve as excellent initial guesses.

We also use an approach, in which low-thrust trajectories are designed by gradually perturbing conic trajectories via a continuation method—a process of converting impulsive maneuvers into low-thrust arcs. While this continuation method requires a number of iterations in the optimization run, being able to capitalize on the wealth of available patched-conic trajectories (which appear in the literature) is an advantage. This method is particularly beneficial when we expect the low-thrust solution to be close to the conic solution.

To facilitate the design process of finding promising trajectories and then to optimize them, we make use of the Satellite Tour Design Program (STOUR)¹⁵⁻¹⁹ and the Gravity Assist Low-thrust Local Optimization Program (GALLOP).²⁰⁻²¹ STOUR was originally developed by the Jet Propulsion Laboratory (JPL) at California Institute of Technology for the mission design of the Galileo tour of Jupiter and was later enhanced at Purdue University to incorporate such capabilities as automated propagation of pure-gravity-assist, aero-gravity-assist, and low-thrust gravity-assist trajectories. GALLOP, which was developed at Purdue University for JPL (based on earlier work by Sims and Flanagan²³), models low-thrust arcs as series of impulses connected by conics and either maximizes the final spacecraft mass or minimizes the initial mass.

A. Exponential Sinusoids as Initial Guesses

By using STOUR-LTGA (for Low Thrust, Gravity Assist) developed by Petropoulos and Longuski, we patch conics and exponential-sinusoid arcs to simulate low-thrust trajectories for the following paths: Earth-Mars-Jupiter (EMJ), Earth-Venus-Earth-Jupiter (EVEJ) and Earth-Earth-Mars-Jupiter (EEMJ). These solutions are then used as initial guesses in the optimization. In the GALLOP solutions, some of the optimization variables, such as flyby dates, are frozen to allow quick comparisons with the original exponential-sinusoid case. The converged solutions are thus considered intermediate for mission purposes (even though they are feasible and optimal in the mathematical sense); and further bootstrapping is necessary to make them meet the hardware and mission requirements for Jupiter rendezvous missions (assuming JIMO spacecraft hardware).

Figure 1 shows a variety of potential EMJ missions during the launch period between January 2010 and December 2044 with an increment of 60 days. In this search, we only look for missions with a total TOF of 6.3 years or less. The Earth launch V_{∞} range is 3 to 6 km/s with an increment of 0.5 km/s, and the average and

maximum accelerations (for the low-thrust engine) are 0.11 mm/s^2 and 0.25 mm/s^2 , respectively. We note that during the initial-search phase, it is unnecessary to match the acceleration values and the hardware. In fact, we often allow much higher accelerations for the STOUR search, knowing that these apparent constraint violations are often repaired during the optimization process by allowing the variables (e.g. flyby dates) to move freely. In the left plot in Fig. 1, attractive candidates are in the left bottom corner because of their low propellant-mass fractions and their low TOF. Further inspection is necessary, however, as not all cases will converge in the optimizer.

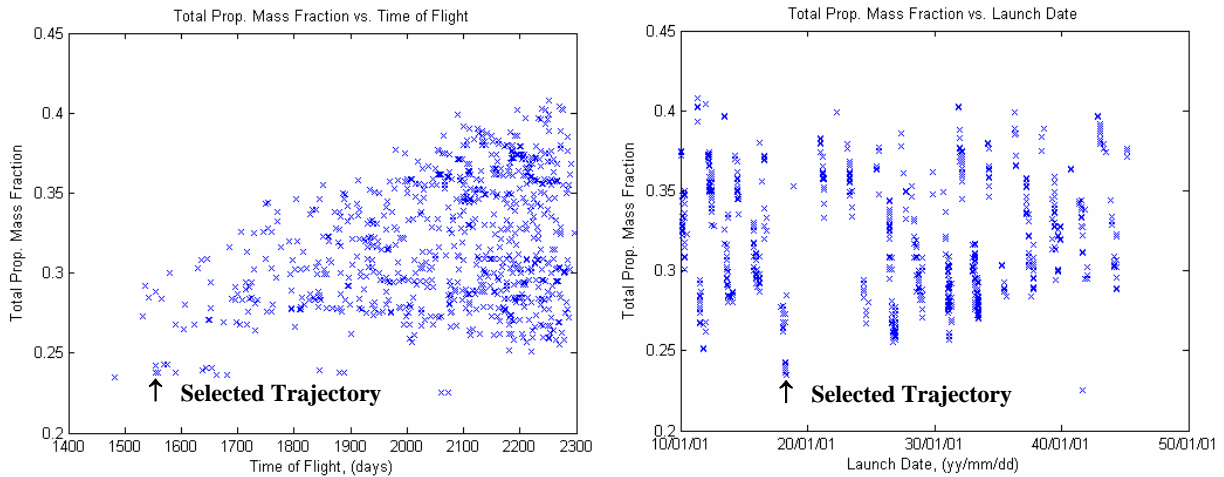


Fig. 1 Exponential Sinusoid Trajectories with the Earth-Mars-Jupiter path (with an Earth launch between January 2010 and December 2044). There are over 400 unique trajectories in the data.

In Fig. 1, the plot on the right has the same vertical axis, a propellant-mass fraction (PMF) ranging between 0.20 and 0.45, but shows how potential missions are distributed over the 35-year launch dates. We see that collections of trajectories appear as nearly vertical lines, suggesting that the EMJ missions repeat approximately every 2 years, the synodic period of Earth and Mars. (We will see later, however, that the EMJ trajectories launched in different opportunities are often of different types and that the eccentricity of Mars and phasing of Jupiter cause considerable variations in the TOF and propellant mass fraction.)

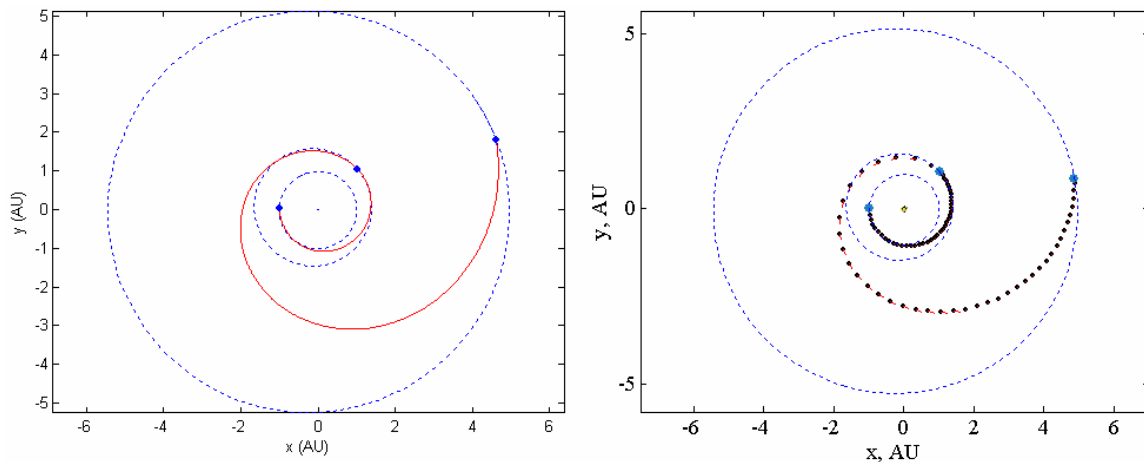


Fig. 2 Trajectory plots of an Earth-Mars-Jupiter mission launched in 2018. STOUR-LTGA (on the left) assumes the shape of exponential sinusoid, whereas GALLOP optimizes the propellant by approximating a low-thrust arc as a series of impulses indicated by the small line segments.

Figure 2 shows trajectory plots of solution found by STOUR-LTGA and GALLOP, which corresponds to one of the trajectories obtained from our search: a case with a launch date on March 20, 2018, a total TOF of 4.72 years,

and a propellant mass fraction of 0.24 (see Table 2). We see how well the exponential sinusoid in STOUR-LTGA serves as an initial guess for GALLOP, in which low-thrust arcs are approximated as a series of impulsive ΔV maneuvers. As noted earlier, this GALLOP solution is still intermediate for mission-design purposes, because the launch, flyby and arrival dates are frozen to allow comparison to STOUR-LTGA. (Thus the computed final mass at Jupiter arrival, currently 17,311 kg, will change once we pose hardware and mission constraints.)

Table 2 Comparison of the Trajectory Characteristics between the STOUR-LTGA Initial Guess and the Intermediate GALLOP Solution for the EMJ Mission in 2018

Characteristics	STOUR-LTGA	GALLOP
Launch Date	2018/3/20	2018/3/20
Launch V_{∞} , km/s	3.00	3.00
Mars flyby V_{∞} , km/s	2.37	3.19
Mars flyby altitude, km	434	200
Jupiter Arrival V_{∞} , km/s	3.73	3.31
Propellant Mass Fraction	0.24	0.13
Total TOF, days	1723	1723

Figure 3 shows over 15,000 EEMJ trajectories that are identified by the STOUR-LTGA search. The cases with low PMF and low launch V_{∞} (inside of the Box *A* in the plot) may seem attractive, but our inspections reveals that these trajectories have difficulty converging or have an extremely short (i.e. days to weeks) transfer to the first Earth flyby. An EEMJ mission encountering Earth immediately after the Earth launch has no advantage over an EMJ mission for practical purposes. So this is one of the examples, where we specifically look for cases with sufficiently high launch V_{∞} and sufficiently long TOF to the first flyby. The selected trajectory pointed by the arrows has launch V_{∞} of above 3 km/s, but has relatively low PMF and acceptable TOF.

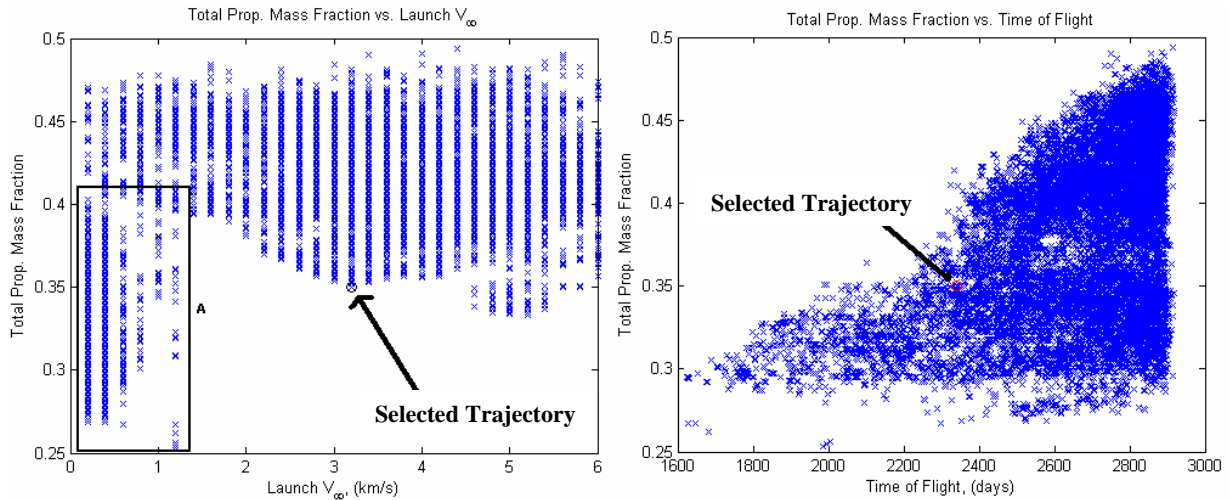


Fig. 3 Exponential Sinusoid Trajectories with the EEMJ path (for the Earth launch between January 2010 and December 2044). There are over 15,000 unique trajectories in the data.

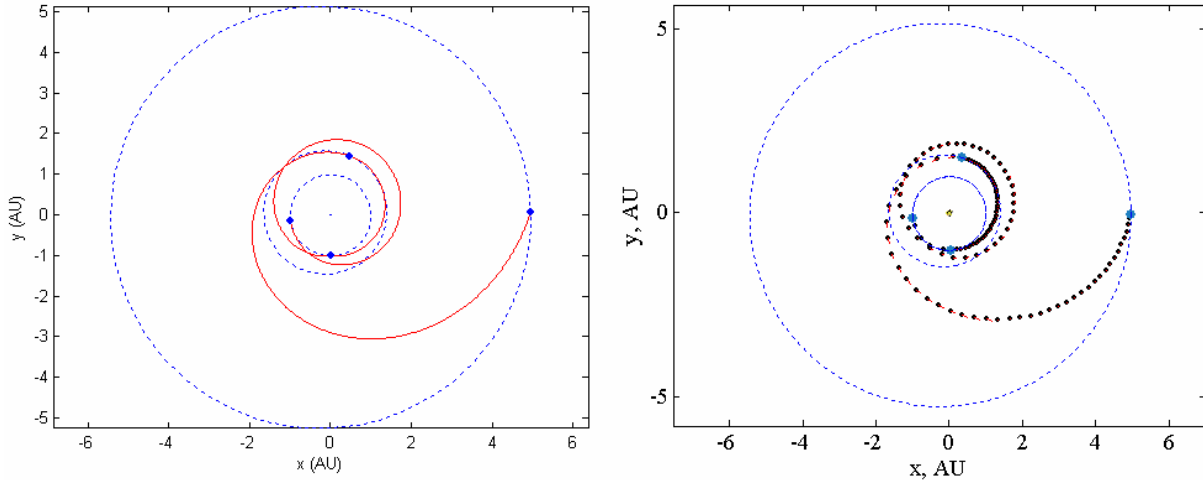


Fig. 4 Comparison of exponential sinusoid (left) and optimized solution for the EEMJ path with an Earth launch in 2016.

In Fig. 4 we have trajectory plots for the selected EEMJ trajectory from STOUR-LTGA and GALLOP. In this converged solution (nevertheless intermediate for the mission purposes) solution on the right, the launch date, the flyby date, and the Jupiter arrival date are frozen. We see that the Earth flyby is not effectively used here, as indicated by the high Earth flyby altitude (Table 3). Again, the Jupiter arrival mass, currently 16,386 kg, will change once subject to hardware and mission constraints and dates are freed.

Table 3 Comparison of the Trajectory Characteristics between the STOUR-LTGA Initial Guess and the Intermediate GALLOP Solution for the EEMJ Mission in 2016

Parameter	STOUR-LTGA	GALLOP
Launch Date	2016/3/30	2016/3/30
Launch V_{∞} , km/s	3.20	3.20
Earth flyby V_{∞} , km/s	4.17	4.02
Earth flyby altitude, km	200	41301
Mars flyby V_{∞} , km/s	2.48	4.04
Mars flyby altitude, km	200	200
Arrival V_{∞} at Jupiter, km/s	4.76	3.90
Propellant Mass Fraction	0.35	0.18
Total TOF, days	2329	2329

Finally, we present two EVEJ trajectories that are selected from the STOUR search and recomputed in the GALLOP optimization. Again, they are intermediate results: in both cases the Earth departure mass are 20,000 kg regardless of the launch V_{∞} , and the Jupiter arrival V_{∞} is unconstrained. To design a mission that is consistent with the hardware and the mission requirements, we use a GALLOP solution (such as the ones presented in this section) as an initial guess for a further bootstrapping. The technique of using a known solution to obtain a near-by solution can be taken to its extreme, in which low-thrust trajectory is designed from a conic solution via a number of iterations.

Table 4 Sample GALLOP Solutions for the EVEJ Paths in 2022 and 2026^a

Parameter	Sample 1	Sample 2
Launch Date, yyyy/mm/dd	2018/8/22	2032/12/26
Launch V_{∞} , km/s	2.19	2.00
Earth-Venus TOF, days	188	133
Venus-Earth TOF, days	347	337
Earth-Jupiter TOF, days	1115	234
Total TOF, years	4.52	3.27
Propellant Mass Fraction	0.22	0.18
Final Mass, kg	15603	16392

^aIn this intermediate result, the spacecraft mass is 20,000 kg regardless of the launch V_{∞} . All dates are frozen.

B. Conic Trajectories as Initial Guesses

We can simulate a patched-conic trajectory in our optimizer by assuming a vehicle with an unrealistically high-acceleration (by assuming a high thrust for a given spacecraft mass or a small mass for a given thrust). Once we have a simulated conic trajectory in our low-thrust optimizer, we then use the solution as initial guess for the next optimization run, except that the spacecraft acceleration for the subsequent run is slightly lower than the previous one. As we repeat this process, the impulsive maneuver is gradually converted into a continuous thrust arc. In some cases, the thrust arcs will fill the entire transfer leg, so that the spacecraft is providing its maximum thrust at all time. To decrease the acceleration even further, we must relax our TOF constraint. Repeating this process of incrementally increasing TOF and decreasing the acceleration, we can eventually obtain a solution for the spacecraft mass consistent with the mission requirements.

The conic initial guesses used in this section are reported by Petropoulos et al. in Ref. 1, in which trajectories to Jupiter are searched assuming a conventional spacecraft that performs ΔV via chemical propulsion. Table 5 shows one of the cases from Ref. 1: the EVVJ trajectory with an Earth launch V_{∞} of 5.00 km/s and a Jupiter arrival V_{∞} of 7.04 km/s. In this conic solution, the spacecraft performs two ΔV impulsive maneuvers of 0.376 km/s and 1.160 km/s during the Venus-Venus leg and the Venus-Jupiter leg, respectively. As we convert this conic solution to a low-thrust trajectory, we also reduce the Jupiter arrival V_{∞} to zero. With our launch vehicle model, the final mass was maximized at the launch V_{∞} of 1.45 km/s. We “pay” for the reduction in the launch and arrival V_{∞} by increasing the TOF by one year, thus fully utilizing the propellant-efficient electric propulsion to achieve a sufficiently high final mass. This process of converting the initial conic solution to the final low-thrust solution took some 30 iterations. (Because the optimizer converges faster if an optimal solution is near the initial guess, we can sometimes reduce the overall computation time with more number of iterations.)

Table 5 Converting a Conic Trajectory into a Low-Thrust Trajectory for the EVVJ Path

Trajectory	Conic ^a	Low-thrust
E1 Launch Date	2031/8/6	2030/12/20
E1 Launch V_{∞} , km/s	5.00	1.45
J4 Arrival V_{∞} , km/s	7.04	0.00
Total TOF, year	4.2	5.2
Final s/c mass, kg	---	15,445

^a Reported in Ref. 1.

There is a clear trade between the launch energy and the TOF: a small launch V_∞ will increase the total TOF, because of the longer TOF required for the Earth-Venus leg, as electric propulsion needs sufficiently long time to achieve the necessary ΔV . The trajectory plot of our EVVJ trajectory is shown in Fig. 5.

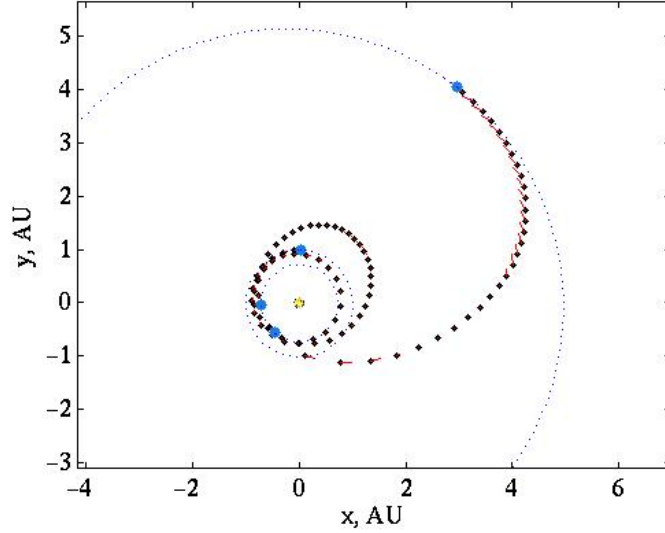


Fig. 5 Earth-Venus-Venus-Jupiter low-thrust trajectory obtained via method of continuation.

Similarly, starting from a conic trajectory, we obtain the following EMJ mission (Table 6). The original conic solution in Ref. 1 has an Earth launch in 2031 and the total TOF of 6.0 years. A conversion to low-thrust mission took about 20 iterations.

Table 6 Converting a Conic Trajectory into a Low-Thrust Trajectory for the EMJ Path.

Trajectory	Conic ^a	Low-thrust ^b
E1 Launch Date	2031/2/12	2030/10/4
E1 Launch V_∞ , km/s	8.00	0.00
J4 Arrival V_∞ , km/s	6.20	0.00
Total TOF, yr	6.0	7.5
Initial s/c mass, kg	---	20,000
Final s/c mass, kg	---	15,757

a. Reported in Ref. 1

b. Launch V_∞ constrained.

III. Variation over Launch Opportunities

There exists direct trajectory to Jupiter every 13 months, the synodic period of Earth and Jupiter. However, a repeatability of a trajectory is less certain when gravity assists are employed. The conic trajectories of the EMJ path, for example, exhibit no clear periodicity as seen in our STOUR search results. To illustrate this point, Fig. 6 shows missions with the launch V_∞ of 4 km/s; no constraints are posed on the Jupiter arrival speed. We see that for the frozen value of launch energy, the launch opportunity does not come often even though we set the minimum flyby altitude to a negative value of -3000 km to allow for the broadest ranges of trajectories. (In fact, all cases shown in this plot involve impractical subsurface flybys.) Similarly, when we consider the launch V_∞ values of 4, 6, and 8 km/s, we find approximately 1,300 trajectories, but only 4 of them has the Mars flyby altitude above 0 km.

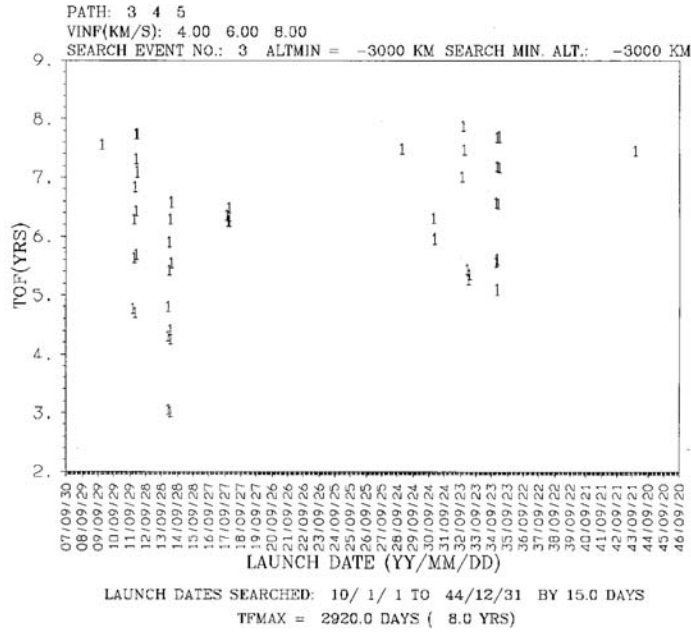


Fig. 6 EMJ Ballistic Trajectories.

Because of electric propulsion’s ability to vary thrust (in magnitude, direction, and duration), raising the flyby altitude above the constraint and adjusting TOF to match the phasing of the planets can be accomplished with additional ΔV . In fact, low-thrust trajectories are so flexible that there are usually more than one trajectory families (with different number of revs) that achieve the same TOF near the launched date (Fig. 7).

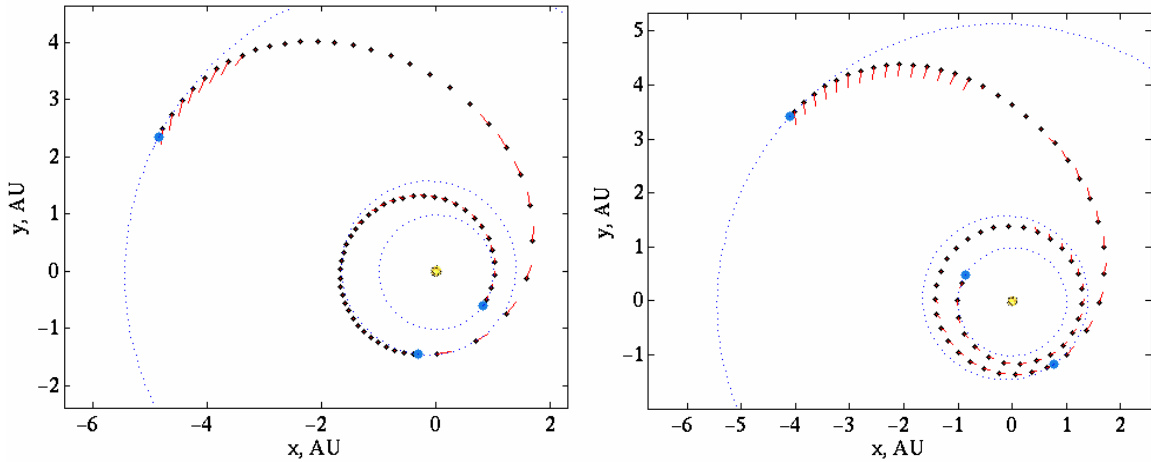


Fig. 7 Two families of EMJ trajectories launched in 2022. TOF is 1800 days (4.93 years) in both cases.

In Fig. 8 we examine performance variations of the EMJ trajectories over different opportunities. Each data in the plot represents a mass-optimal solution for given maximum-TOF constraint (shown on the horizontal axis). As in the studies by Parcher and Sims,²⁻⁴ we see that the final mass usually increases as the TOF increases. Among the launch periods we studied, missions launched in 2022 and 2026 have the final mass greater than the cases in 2031/2032 by more than 1,000 kg. The difference in the final mass is more evident for when tighter TOF

constraints are posed. For example, although the long-leg solutions in 2022 and 2026 have the same final mass at TOF of 6 years, the 2026 case performs poorly when the TOF is reduced to 5.2 years; the difference between these two cases widens to about 2,000 kg (10% of the initial mass). For missions in 2022, the short-leg solution is more effective when the TOF is less than about 5 years. For TOF longer than 5 years, the best performance cases are given by the 2026 short-leg, 2022 long-leg, and 2026 long-leg solutions.

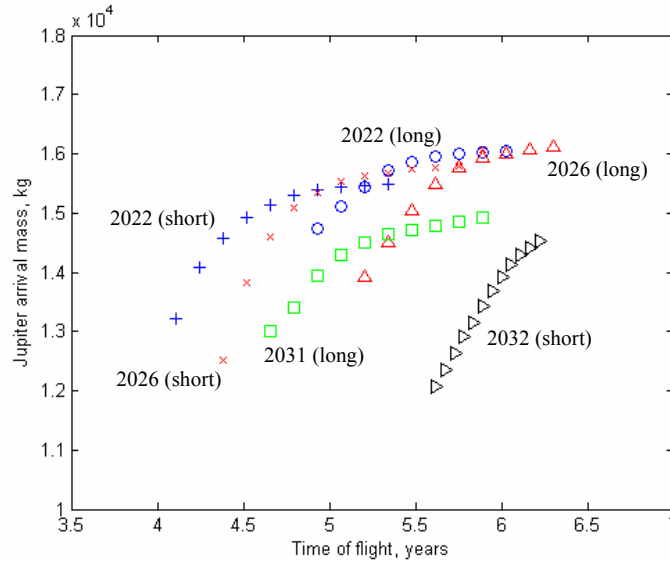


Fig. 8 The performance variations over launch opportunities for the EMJ path. “Short” and “long” indicate whether the Earth-Mars transfer leg is relatively short (with fewer revs) or long (with more revs), as compared in Fig. 7.

IV. Hardware Trade

When we consider an NEP spacecraft, a larger vehicle has a scaling advantage in the nuclear dynamic power system; the specific mass of the power system may be as high as 30-40 kg/kW_e at 100kW_e but as low as 5 kg/kW_e at 100 MW_e.²³ Furthermore, the number of required thrusters, and mass thereof, can be reduced by employing thrusters with higher thrust density. For instance, a single MPD thruster produces thrust on the order of tens of newtons, as opposed to hundreds of milli-newtons for an ion thruster. Thus, to achieve a higher acceleration the assumed vehicle size is usually larger.

Due to the difference in their acceleration (and their I_{sp}), spacecraft of different sizes fly different trajectories. Let us now assume a Jupiter rendezvous mission with a hypothetical NEP vehicle. In Fig. 9 on the left, we have a trajectory plot of an Earth-Venus-Venus-Jupiter trajectory assuming a fictitious spacecraft that is a 26% scaled-down version of JIMO: although the mass is reduced to a quarter of its original size (to fit the payload capacity of an Atlas 531), the thrust and the mass-flow rate are reduced accordingly, so that the resulting trajectory is identical to the one for the full-size JIMO. The bias due to the difference in the launch vehicle is negligible.

In practice, however, the power capability of this smaller spacecraft will be much less than 26% of JIMO due to its higher specific mass. For a spacecraft that could be launched by an Atlas 531, it is probably more realistic to assume a radioisotope electric propulsion (REP) spacecraft with a power level of around 1 kW_e as reported by Bonfiglio et al. in Ref 24. For such a low level of power, thrust can be increased by reducing I_{sp} . When we assume hardware parameters similar to the one reported in Ref. 24, the propellant mass fraction and TOF must increase as shown in Fig. 9 and Table 8.

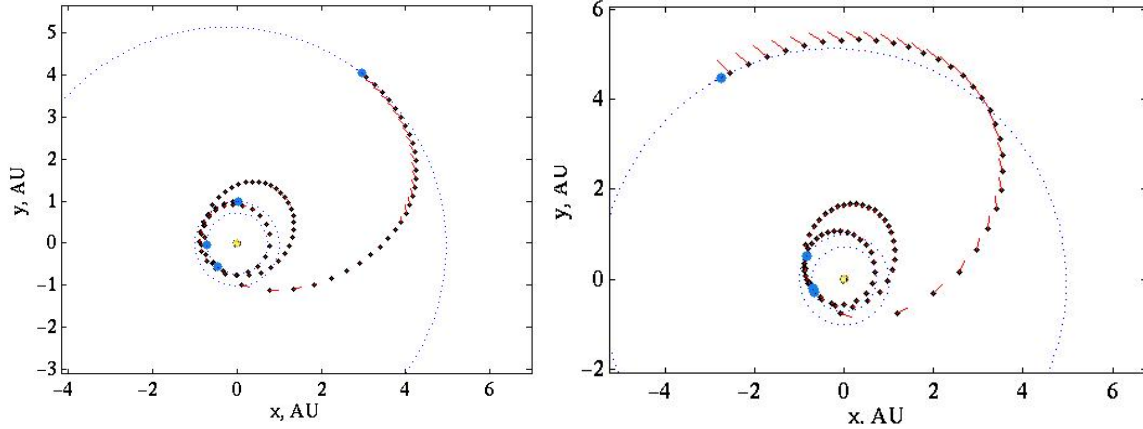


Fig. 9 Earth-Venus-Venus-Jupiter trajectories flown by the JIMO Spacecraft (left) and by a smaller REP Spacecraft (right).

Table 8 Comparison of Mission Characteristics between the “Scaled-Down JIMO Spacecraft” and a Representative REP Spacecraft.^a

	"26% JIMO"	REP
power, kW _e	24.7	1
I_{sp} , s	6000	1783
efficiency	0.7	0.45
thrust, N	0.589	0.051
mass flow rate, kg/s	1.00E-05	2.94E-06
Launch V_{∞} , km/s	1.46	7.57
TOF, years	5.2	8
mf, kg	4025	984

^aAssumed launch vehicle is Atlas 531, which has the capability to inject 5212 kg of payload for launch $V_{\infty}=0$.

In Fig. 10, the “final mass vs TOF trades” for EMJ trajectories are computed for I_{sp} values of 3000, 6000, and 9000 s and for thrusts of 1, 2, and 10 N. For a given I_{sp} and thrust, there appears to be asymptotic limits for the final mass when the TOF is unconstrained. In principle, although not shown on this plot, there is a shortest TOF possible for given spacecraft parameters, which occurs when the engine is thrusting continuously.

In all cases a higher I_{sp} results in a higher final mass. But at high I_{sp} values, there are diminishing returns (especially when the acceleration is low). For example, there is little difference in m_f for I_{sp} between 6000 and 9000 s for the 1-N case.

Since m_o is kept the same for all three thrust levels, a higher thrust results in a higher acceleration. However, we note that a higher thrust for the same mass is tantamount to assuming lower specific mass, or equivalently, assuming more advanced technologies. (As we have noted, a more massive spacecraft provides lower specific mass for the same level of technology.)

Similar trends are observed for the EVEJ path (as shown in Fig. 11). We see that the m_f -TOF curve shifts upwards and to the left as I_{sp} and accelerations are increased. (The original curve for the JIMO spacecraft is plotted for comparison.)

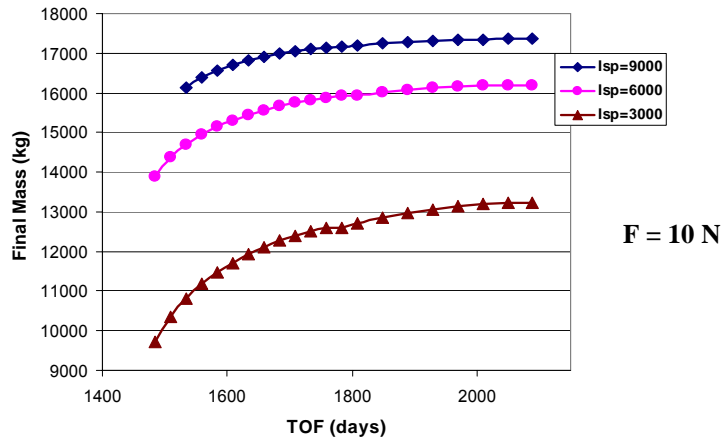
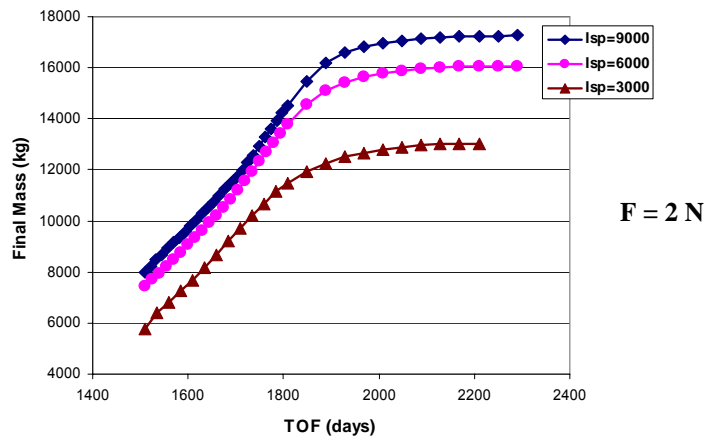
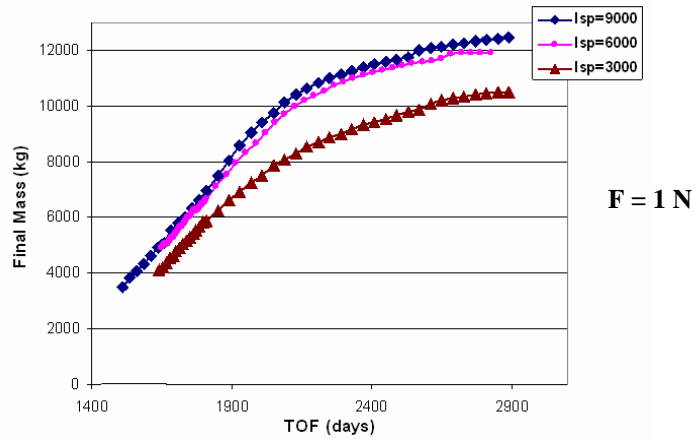


Fig. 10 Variations of the final mass for the EMJ trajectory due to variations in the hardware parameters.

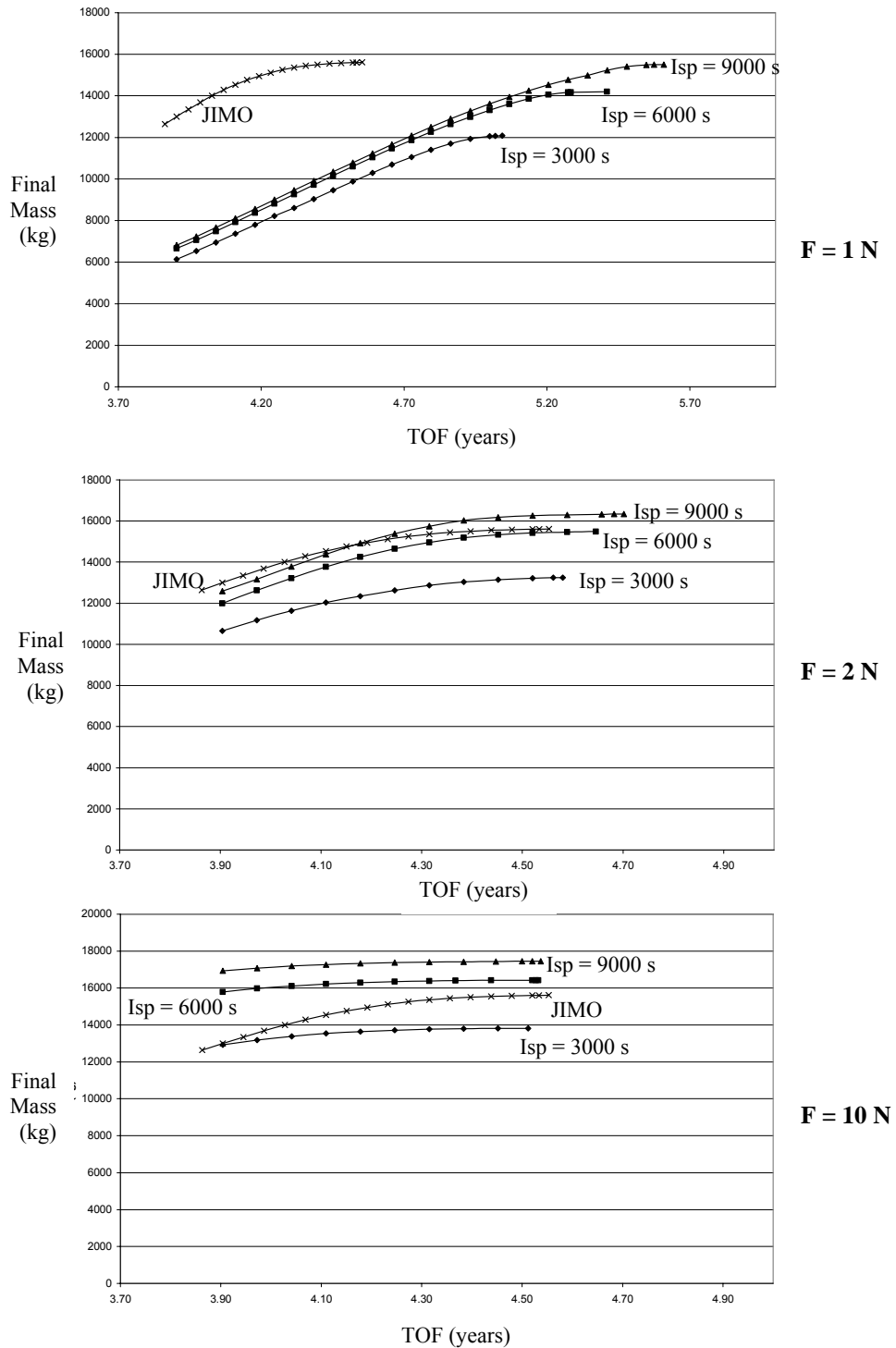


Fig. 11 Variations of the final mass for the EVEJ trajectory due to variations in the hardware parameters. For the JIMO spacecraft: $F=2.26\text{ N}$, $I_{sp} = 6000\text{ s}$.

V. Conclusion

In this paper we present low-thrust trajectories to Jupiter for Earth launch between 2010 and 2045. We use exponential-sinusoid arcs and conic arcs as initial guesses to obtain EMJ, EEMJ, EVVJ, and EVEJ trajectories. The performance of trajectories involving intermediate flybys varies considerably depending on the mission year (except when the flyby body involves only Earth); in the EMJ case, for example, slips in launch date cause m_f variations on the order of 15% of m_o or TOF variations of several months to a year. Our m_f -TOF trade studies exhibit an expected trend, in which the final mass increases when the TOF is relaxed, but m_f approaches an asymptotic limit. A higher I_{sp} helps increase the final mass, although there is a point of diminishing return at a high I_{sp} value especially when the acceleration is low. The propellant mass can be reduced by a higher acceleration (where the mass and I_{sp} are held fixed). This improvement is more evident for cases with tighter TOF constraints. For a given spacecraft mass, the higher-acceleration solutions correspond to higher-technology levels; if the present-day technology is assumed, an increase in the spacecraft size is necessary to achieve a mission requiring low propellant-fraction and short time of flight.

Acknowledgments

This work is supported in part by the Jet Propulsion Laboratory (JPL), California Institute of Technology, under Contract 1250863 (Jon A. Sims, Technical Manager). We thank Slawomir Boruch, Megan Darraugh, James Garner, Steven McNutt, and Daniel Miller for their contributions.

References

- ¹ Petropoulos, A. E., Longuski, J. M., and Bonfiglio, E. P., "Trajectories to Jupiter via Gravity Assists from Venus, Earth, and Mars," *Journal of Spacecraft and Rockets*, Vol. 37, No. 6, Nov-Dec. 2000.
- ² Parcher, D. W. and Sims, J. A., "Earth Gravity-Assist Trajectories to Jupiter Using Nuclear Electric Propulsion," AAS/AIAA Astrodynamics Specialist Conference, AAS Paper 05-397, Lake Tahoe, CA, Aug. 7-11, 2005.
- ³ Parcher, D. W. and Sims, J. A., "Gravity-Assist Trajectories to Jupiter Using Nuclear Electric Propulsion," AAS/AIAA Astrodynamics Specialist Conference, AAS Paper 05-398, Lake Tahoe, CA, Aug. 7-11, 2005.
- ⁴ Parcher, D. W. and Sims, J. A., "Venus and Mars Gravity-Assist Trajectories to Jupiter Using Nuclear Electric Propulsion," AAS/AIAA Astrodynamics Specialist Conference, AAS Paper 05-112, Copper Mountain, CO, Jan. 23-27, 2005.
- ⁵ Greeley, R. and Johnson, T., Ed., "Report of the NASA Science Definition Team for the Jupiter Icy Moons Orbiter", NASA Science Definition Team, Feb. 2004.
- ⁶ Whiffen, G. J., "An Investigation of a Jupiter Galilean Moon Orbiter Trajectory", AAS/AIAA Astrodynamics Specialist Conference, AAS Paper 03-554, Big Sky, Montana, Aug. 3-7, 2003.
- ⁷ Greeley, R. and Johnson, T., Ed., "Report of the NASA Science Definition Team for the Jupiter Icy Moons Orbiter", NASA Science Definition Team, Feb. 2004.
- ⁸ Polk, J. E., Goebel, D., Brophy, J. R., Beatty J., Monheiser, J., Giles D., Hobson D., Wilson, F., Christensen, J., De Pano M., Hart, S., Ohlinger W., Hill D. N., Williams, J., Wilbur, P. and Farnell, C., "An Overview of the Nuclear Electric Xenon Ion System (NEXIS) Program", AIAA-2003-4713, Joint Propulsion Conference, Huntsville, AL, July 20-23, 2003.
- ⁹ Yam, C. H., McConaghy, T. T., Chen, K. J., and Longuski, J. M., "Preliminary Design of Nuclear Electric Propulsion Missions to Outer Planets," AIAA/AAS Astrodynamics Specialist Conference, AIAA Paper 2004-5393, Providence, RI, Aug. 16-19, 2004.
- ¹⁰ Rayaman, M. D., Varghese, P., Lehman, D. H., and Livesay, L. L., "Results from the Deep Space 1 Technology Validation Missions," *Acta Astronautica*, Vol. 47, Nos. 2-9, 2000, pp. 475-487.
- ¹¹ Petropoulos, A. E., Longuski, J. M. and Vinh, N. X., "Shape-Based Analytic Representations of Low-Thrust Trajectories for Gravity-Assist Applications," AAS/AIAA Astrodynamics Specialist Conference, AAS Paper 99-337, Girdwood, Alaska, Aug. 1999. Also in *Advances in the Astronautical Sciences*, Univelt Inc., San Diego, CA, Vol. 103, Part I, 2000, pp. 563-581.
- ¹² Petropoulos, A. E. and Longuski, J. M., "Automated Design of Low-Thrust Gravity-Assist Trajectories," AIAA/AAS Astrodynamics Specialist Conference, AIAA Paper 2000-4033, Denver, Colorado, Aug. 2000. *A Collection of Technical Papers*, American Institute of Aeronautics and Astronautics, Reston, Virginia, pp. 157-166.
- ¹³ Petropoulos, A. E. and Longuski, J. M., "A Shape-Based Algorithm for the Automated Design of Low-Thrust, Gravity-Assist Trajectories," AAS/AIAA Astrodynamics Specialist Conference, AAS Paper 01-467, Quebec City, Canada, July-Aug. 2001.
- ¹⁴ Petropoulos, A. E., "A Shape-Based Approach to Automated, Low-Thrust, Gravity-Assist Trajectory Design," Ph.D. Thesis, School of Aeronautics and Astronautics, Purdue University, West Lafayette, IN, May 2001.
- ¹⁵ Rinderle, E. A., "Galileo User's Guide, Mission Design System, Satellite Tour Analysis and Design Subsystem," Jet Propulsion Laboratory, California Institute of Technology, JPL D-263, Pasadena, CA, July 1986.
- ¹⁶ Williams, S. N., "Automated Design of Multiple Encounter Gravity-Assist Trajectories," Master's Thesis, School of Aeronautics and Astronautics, Purdue University, West Lafayette, IN, Aug. 1990.
- ¹⁷ Longuski, J. M. and Williams, S. N., "Automated Design of Gravity-Assist Trajectories to Mars and the Outer Planets," *Celestial Mechanics and Dynamical Astronomy*, Vol. 52, No. 3, 1991, pp. 207-220.
- ¹⁸ Patel, M. R. and Longuski, J. M., "Automated Design of Delta-V Gravity-Assist Trajectories for Solar System Exploration," AAS Paper 93-682, B.C., Canada, Aug 1993.

- ¹⁹ Bonfiglio, E. P., and Longuski, J. M., "Automated Design of Gravity-Assist and Aerogravity-Assist Trajectories," *The Journal of Spacecraft and Rockets*, Vol. 37, No. 6, 2000, pp. 768-775.
- ²⁰ McConaghy, T. T., "Design and Optimization of Interplanetary Spacecraft Trajectories," Ph.D. Thesis, School of Aeronautics and Astronautics, Purdue University, West Lafayette, IN, Dec. 2004.
- ²¹ McConaghy, T. T., Debban T. J., Petropoulos, A. E., and Longuski, J. M., "Design and Optimization of Low-Thrust Trajectories with Gravity Assists," *Journal of Spacecraft and Rockets*, Vol. 40, No. 3, 2003, pp. 380-387.
- ²² Sims, J. A., and Flanagan, S. N., "Preliminary Design of Low-Thrust Interplanetary Missions," AAS/AIAA Astrodynamics Specialist Conference, AAS Paper 99-338, Girdwood, Alaska, Aug. 1999. Also in *Advances in the Astronautical Sciences*, Univelt Inc., San Diego, CA, Vol. 103, Part I, 1999, pp. 583-592.
- ²³ Frisbee, R. H., "Advanced Space Propulsion for the 21st Century," *Journal of Propulsion and Power*, Vol. 19, No. 6, Nov.-Dec. 2003.
- ²⁴ Bonfiglio, E. P., Oh, D., and Yen, C. W., "Analysis of Chemical, REP, and SEP Missions to the Trojan Asteroids," AAS Paper 05-396, AAS/AIAA Astrodynamics Conference, Lake Tahoe, CA, Aug. 7-11, 2005.